DEVELOPMENT OF A 100 WATT S-BAND TRAVELING-WAVE TUBE

By

L. A. Roberts
M. V. Purnell

9 August 1967

Contract No. 951299

This work was performed for the Jet Propulsion Laboratory, California Institute of Technology, sponsored by the National Aeronautics and Space Administration under Contract NAS7-100.

Quarterly Report No. 4

Watkins-Johnson Company
3333 Hillview Avenue
Palo Alto, California

ABSTRACT

This report is the fourth quarterly progress report on the development of the WJ-395, a 100 watt, 55 percent efficiency, 2.3 GHz traveling-wave tube for space applications. During this quarter random and sinusoidal vibration performance tests were made on Tube S/N 3 and excellent results were obtained. A two-helix tube was built and tested. Because of internal helix loss problems resulting from constructional difficulties, the tube did not give good electrical performance. A single-helix tube was built operating at a design perveance of 0.80×10^{-6} which gave excellent efficiency results at 66 and 100 watts. Overall efficiency of 45.2 percent was achieved. This tube also incorporated the new collector design.

TABLE OF CONTENTS

LIST OF ILLUSTRATIONS

LIST OF ILLUSTRATIONS (Continued)

LIST OF ILLUSTRATIONS (Continued)

I. INTRODUCTION

Purpose and Goals of the Project

The purpose of this program is to develop a high efficiency, 100 watt, 2.3 GHz traveling-wave tube suitable for use in space. The tube has been designated the WJ-395. The most important goal of the program, requiring an advance over present techniques, is the achievement of high efficiency. The basic performance goals are a power output of 100 watts at an overall efficiency of 55 percent and a gain of 30 dB. Other requirements dictate conduction cooling and the ability to perform through launch and under space environment conditions.

Basis for High Efficiency Designs

At the time of the contract award, excellent results had been achieved on a program of research into high efficiency traveling-wave tube techniques at Watkins-Johnson. This program, supported by the Evans Laboratory of the U. S. Army Electronics Command under Contract No. DA-28-043AMC-02004(E) had been underway for some time. In the course of the USAECOM program, a helix-type traveling-wave tube was built which yielded an overall efficiency of 51 percent with 20 watts output at 1.0 GHz. This was done using a "two helix approach" wherein a signal is amplified and extracted from a first section of a tube and reinserted into an attenuatorless helix section at the output which can be operated at a different voltage. The output signal of the tube is taken from the second helix section and the electron beam is dissipated in a depressed collector.

Another technique which subsequently demonstrated comparable efficiencies (i.e., greater than 50 percent) with a single helix voltage has also evolved from the USAECOM program. This is called the "positive taper helix" approach. This technique involves a combination of large overvoltage operation of the helix and an increased helix pitch at the output end of the helix (in contrast to the conventional "negative" taper).

A company-sponsored research program has been initiated to explore the helix and beam design parameters which control high efficiency performance. The main purpose is to gain an understanding which will allow accurate scaling of high efficiency tubes in both frequency and power level. This study is also taking place at 1.0 GHz using basically the same electron beam, vacuum envelope, rf structure and magnetic field system as the USAECOM program. Results from this program are beginning to yield information as to the controlling parameters on high efficiency and have

pointed to avenues of exploration which might lead to even higher efficiency values. The design parameters of tubes from this program have been applied to the WJ-395 and have yielded excellent efficiency results which will be discussed in this report.

This present program for a 100 watt tube and a parallel program for NASA Langley Research Center to study means of achieving very high efficiencies with the WJ-274, are designed to apply these techniques to a PPM focused, space type TWT. The JPL and Langley tubes represent hardware with intended spacecraft use.

Purpose of Early Tubes

The purpose of the early tubes (S/N 1, 2, 3 and 4) was primarily to establish the electrical, mechanical and thermal design of the basic tube. The magnetic structure was worked out and evaluated for temperature stability. Comparative evaluation was made of glazed vs clamped rod helix structures from the standpoint of efficiency. Random and sinusoidal vibration tests established the validity of the mechanical design and have shown that incidental AM and PM were within specifications and that the encapsulation scheme was consistent with these. Reasonable efficiency and gain performance were demonstrated, i.e., 35 percent overall efficiency and 33 dB gain at the 100 watt level, to indicate that a good test vehicle had been established for the subsequent efficiency improvement effort.

General Tube Construction

The general tube construction is metal-ceramic. An exploded view of the tube and its subassemblies is shown in Fig. 1. An exploded view of the gun subassembly is shown in Fig. 2. An exploded view of the collector used on the first five tubes is shown in Fig. 3.

II. EXPERIMENTAL PROGRAM

WJ-395 S/N 3

Vibration Tests

Phase modulation measurements were made while tube S/N 3 was being vibrated. The dynamic phase measurements were made with the circuit shown in Fig. 4. This circuit is diagramed here because it proved to be very satisfactory and was free of spurious responses or residual noise. With the

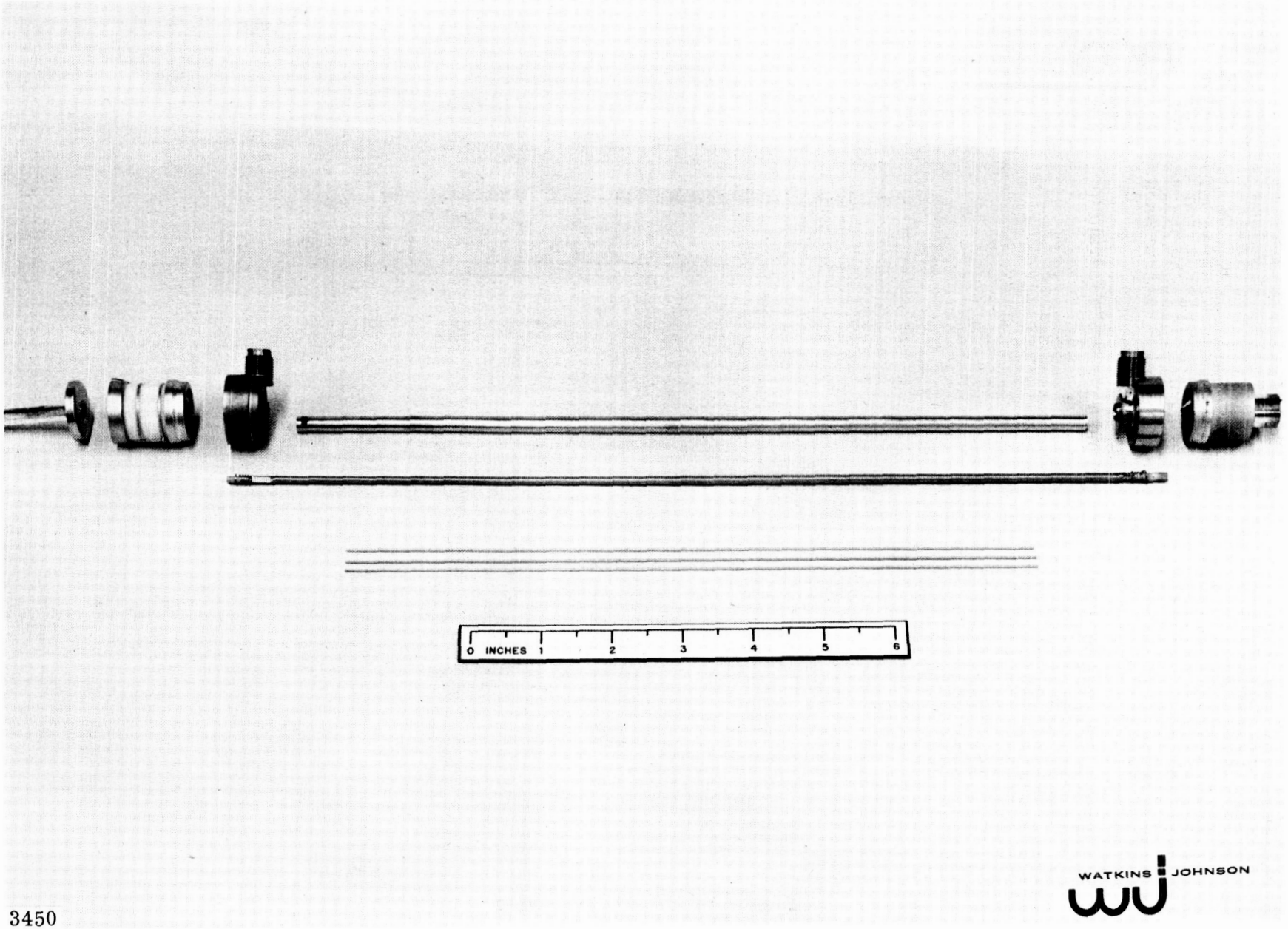

Fig. 1 - Photograph of an exploded view of the tube subassemblies showing the electron gun on the left, the barrel and helix (center) and the collector on the right.

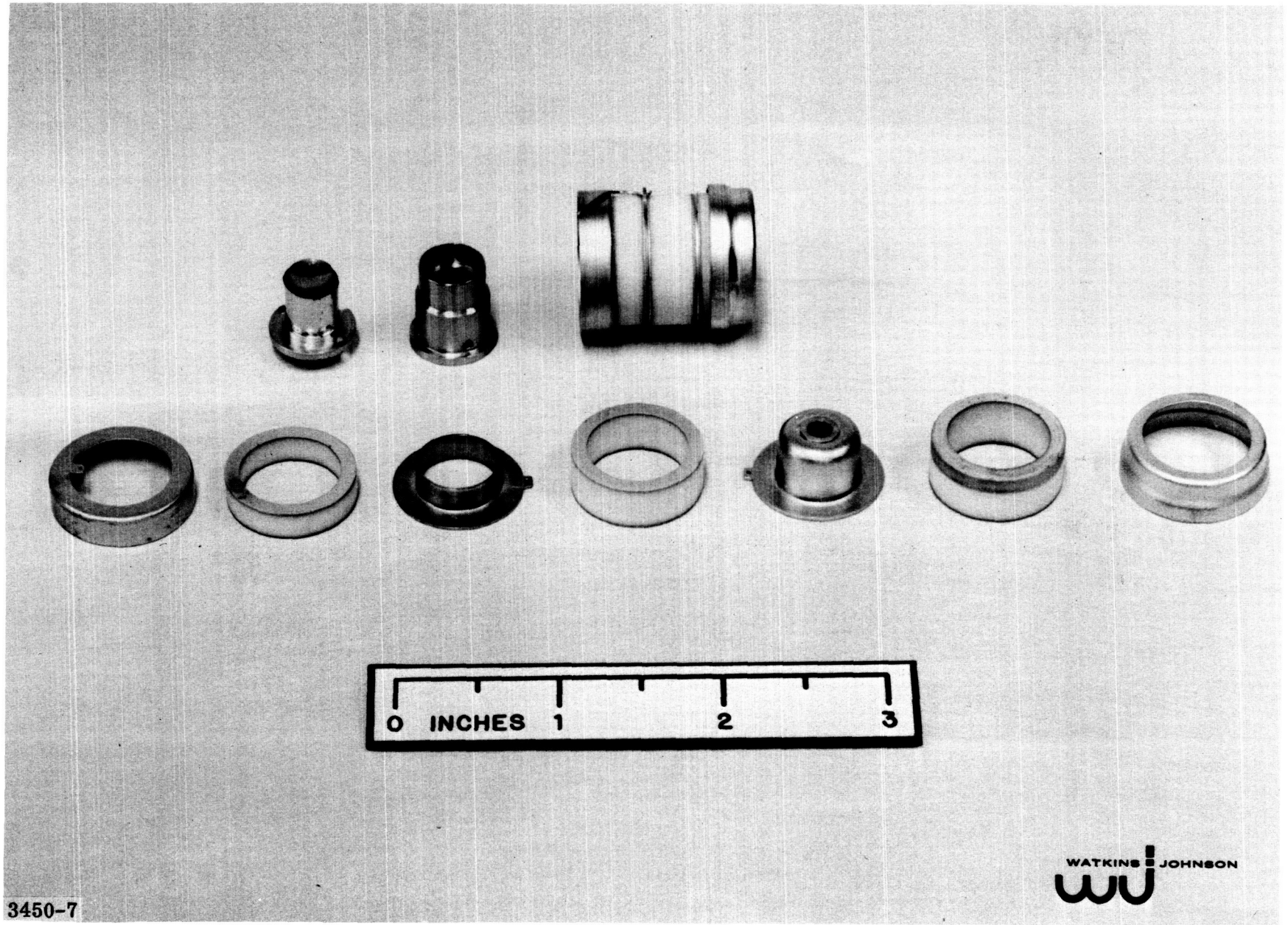

Fig. 2 - Photograph showing an exploded view of the electron gun subassembly. Foreground shows the metal-ceramic parts comprising the insulator, vacuum-envelope structure (right rear). The focus-electrode is at center rear and the cathode subassembly is at the left rear. See also Fig. 8 in Quarterly Report No. 1.

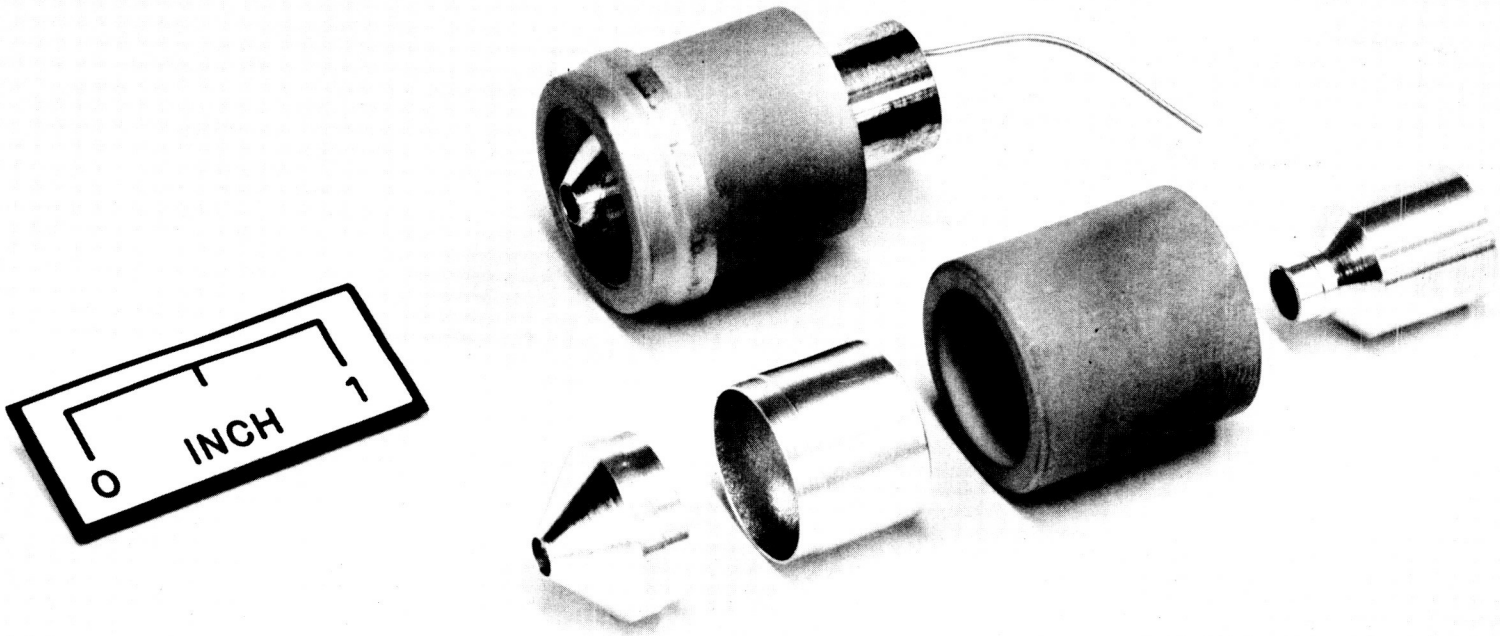

WATKINS JOHNSON

3450-4

Fig. 3 - Photograph showing an exploded view of parts used on the collector subassembly (rear) used on tubes S/N 1 through 5. See also Fig. 9 in Quarterly Report No. 1.

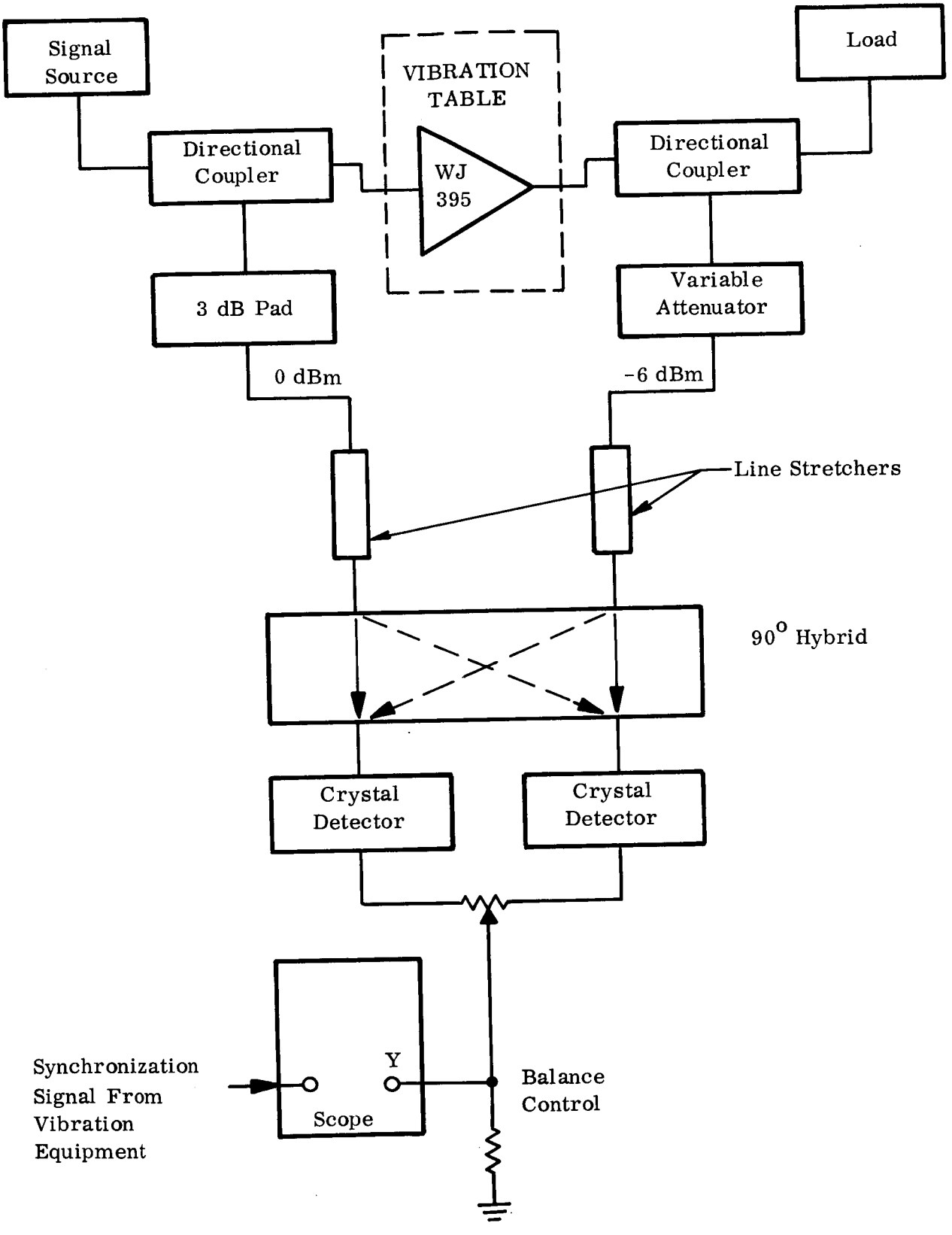

Fig. 4 - Block Diagram of dynamic phase measuring equipment used during vibration tests.

relative signal levels shown, the phase indication is relatively insensitive to output level changes of the tube. The $\pm 90^{o}$ calibration and zero balance can be readily accomplished with the combined adjustment of the line stretchers, the balance control and the scope gain. Phase changes of 0.05^{o} could be measured.

The tube was sinusoidally vibrated over the 15 cps to 2kc range at the 5G level in each of three planes. The maximum peak phase excursion of 0.2^{o} was observed between 1 and 2 kc. This amounts to a value of 0.04 degrees per peak G. The specifications allows 0.5^{o}/pk G.

The tube was placed in random vibration with flat equalization of the spectral power density over the frequency range of 15 to 2000 cps. Amplitude modulation was monitored with a crystal detector. The first tests were at a 14 G rms level for 5 minutes in each plane. Spectral power density (SPD) was 0.098 g^2/cps. The second tests were at a 20 G rms level for 10 minutes in each plane. The SPD was 0.2 g^2/cps. The third tests were with random + sine drive in the axial direction only. The level was 9.0 G rms sine wave over the range of 40 to 2000 cps superimposed on 5.0 G rms random equalized as above. Some AM was observed during these tests. It was subsequently found to be due to a faulty input cable. The 20 G rms random tests were repeated for 15 minutes each in the axial and one transverse plane. In the transverse plane, no AM could be observed at saturation and 0.09 dB peaks could be measured with the drive adjusted for power output to be 1.0 dB below saturation. In the axial plane, 0.09 dB peaks could be measured at saturation and 0.23 dB peaks could be measured at 1.0 dB down on the output.

Conclusions on the Vibration Tests

From these vibration tests it can be concluded that the mechanical design of the tube from the standpoint of motion of the elements and resonances is more than adequate to meet the electrical requirements. In addition, the duration and amplitude of the random vibration tests far exceeded the specification requirements. The specification requirements are:

14 G rms for 18 seconds;
5 G rms noise + 2 G rms sine 15-40 cps, then
5 G rms noise + 9 G rms sine 40-2000 cps for a total of 600 seconds;
14 G rms noise for 18 seconds.

The random test time was 15 minutes at the 14 G rms level and 60 minutes additional test time at the 20 G rms level. It is felt that sufficient random tests were performed to find mechanical fatigue failures, none of which occurred.

WJ-395 S/N 5

Design Basis for the Two-Helix Tube

The design of the two-helix tube was based upon a scaling of the second Niclas-Gerchberg two-helix tube. Since scaling had to be accomplished in both power level and frequency, certain choices has to be made as to which normalized parameters would be held constant.

The most difficult operating characteristics to predict under large overvoltage operation are the small signal and saturation gain. Since the tube which is being scaled and the tube from which it is being scaled have close to the same values of C, N and γa, gain was chosen to be the same under the conditions of small signal synchronism. This makes the assumption that the gain will decrease under overvoltage conditions in the same way. This is a reasonable assumption under the conditions of the similar parameters mentioned above. The other parameter which was chosen to be the same was the overvoltage parameter b'. Other choices which had to be made, based upon power output requirements and focusing capabilities, were power output of 100 watts, beam efficiency of 30 percent and an operating beam perveance of 0.80×10^{-6}. With these conditions chosen and in addition using known dispersion curves for this general helix type, the design of the tube was defined.

Fig. 5 shows the layout of the body and window design and the associated helix, attenuator and drift space design. The helices are rod supported with respect to the barrel with beryllium oxide rods. The first stage helix (the sections at 28.2 TPI) is operated at body potential. The helix sections are physically welded to the body at the 1st sever. The second stage of the helix (25.5 TPI) is unattenuated and is completely insulated from the body so that it can be operated at an arbitrary potential. A photograph of the tube is shown in Fig. 6.

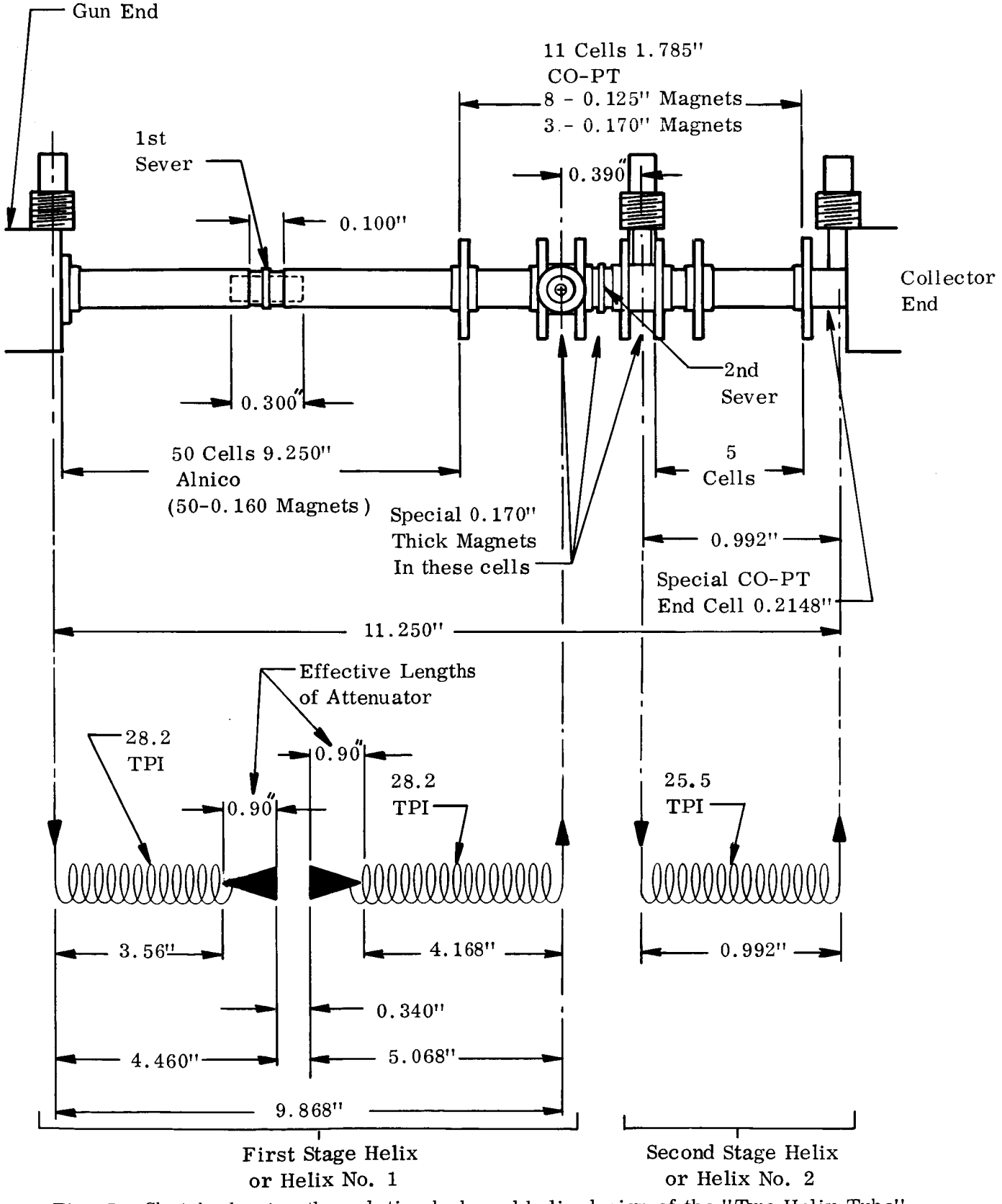

Fig. 5 - Sketch showing the relative body and helix design of the "Two Helix Tube", WJ-395 S/N 5. **Most of the polepieces have been eliminated for clarity.**

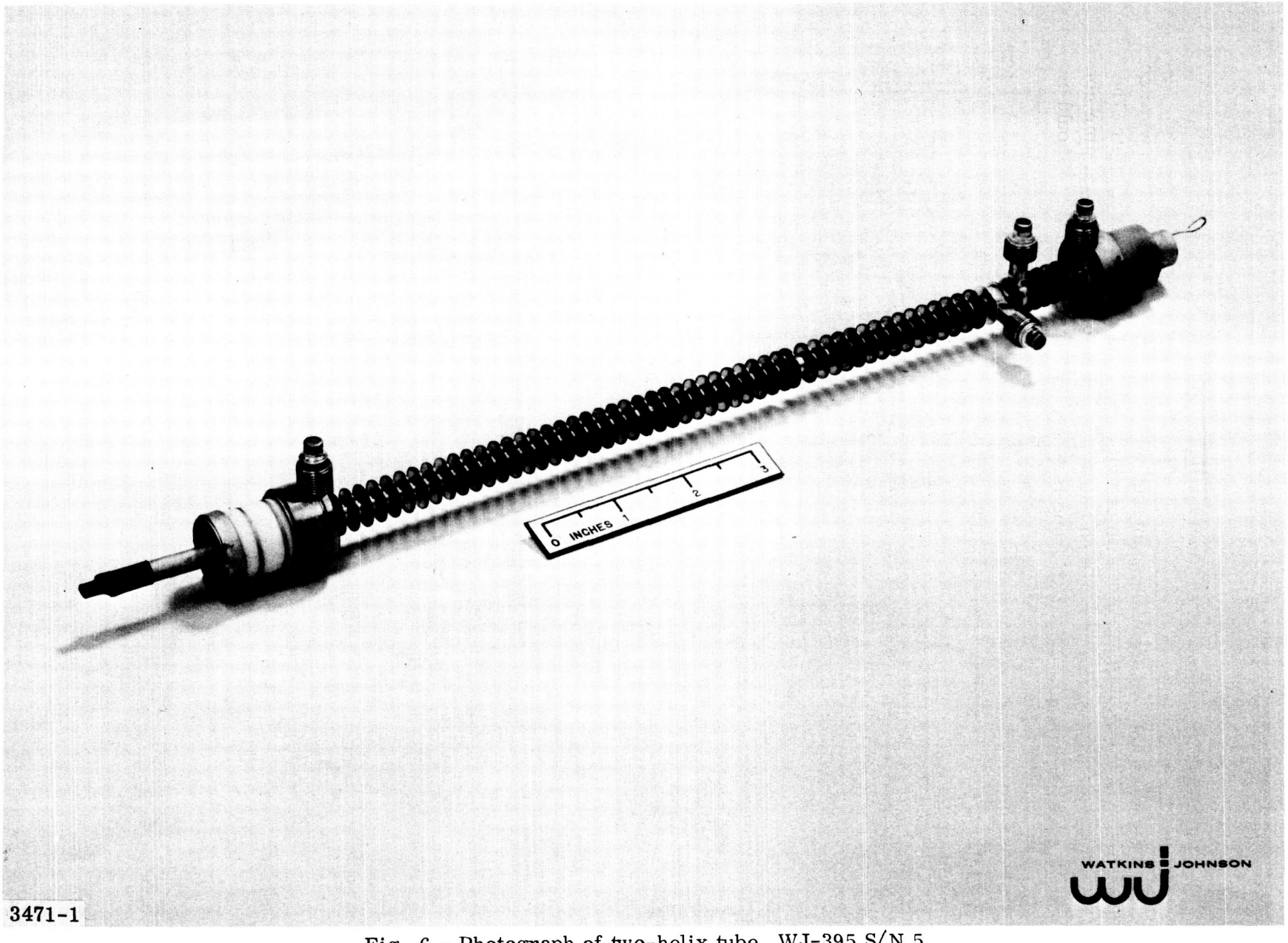

Fig. 6 - Photograph of two-helix tube, WJ-395 S/N 5.

Problems Encountered on the Two-Helix Tube

Several problems were encountered with this tube, some of which were construction difficulties and some of which involved rf characteristics. The construction of the tube turned out to be much more difficult and time-consuming than anticipated. If another tube is to be built, certain changes should be incorporated which were realized during the construction but which could not be incorporated without a major change in construction and additional assembly technique experiments. These will be discussed later.

The rf problem which was most detrimental to tube performance was the helix loss problem. This occurred during brazing assembly and vacuum bakeout of the tube. Because of the difficult heating problem during the bell-jar braze at the second sever (see Fig. 5), the body was overheated and an excess of the silver-bearing brazing alloy flowed into the interior of the tube. During vacuum bakeout of the tube, the vapor pressure of the brazing alloy exceeded the vacuum level within the tube, and silver evaporated and deposited on the support rods of the helix. This thin layer of metallic silver introduced sufficient loss to markedly change the expected efficiency performance of the tube. The loss which can be expected on an unattenuated section of helix of the type used in this tube is 0.15 dB per wavelength. Fig. 7 shows the measured loss of the "second stage" or output section of helix compared with the loss calculated from the above value of 0.15 dB/λg. The same sort of increase in loss is most certainly on the output end region of the "first stage" helix section. This cannot be measured directly. This also leads to a decrease in efficiency of this section.

The presence of the metallic film on the helix support rods after bakeout also led to a dc leakage path from the "second stage" helix to the body. This was measured to be approximately 100,000 ohms and would lead to 1.0 mA of current flow for each 100 volts of difference voltage between body and helix. This was eventually cleared by passing a large current through this leakage path, but the rf loss still remained.

One further difficulty which was found to occur during operation of the tube involved emission of secondary electrons from the helices on either side of the second sever. This occurred whenever a potential difference was applied between the helices. This effect was not observed on the Niclas-Gerchberg two-helix tubes because of the stiffer solenoid focusing employed. In this PPM focused case, the increase of primary helix current interception associated with large signal operation of the tube causes the release of secondary

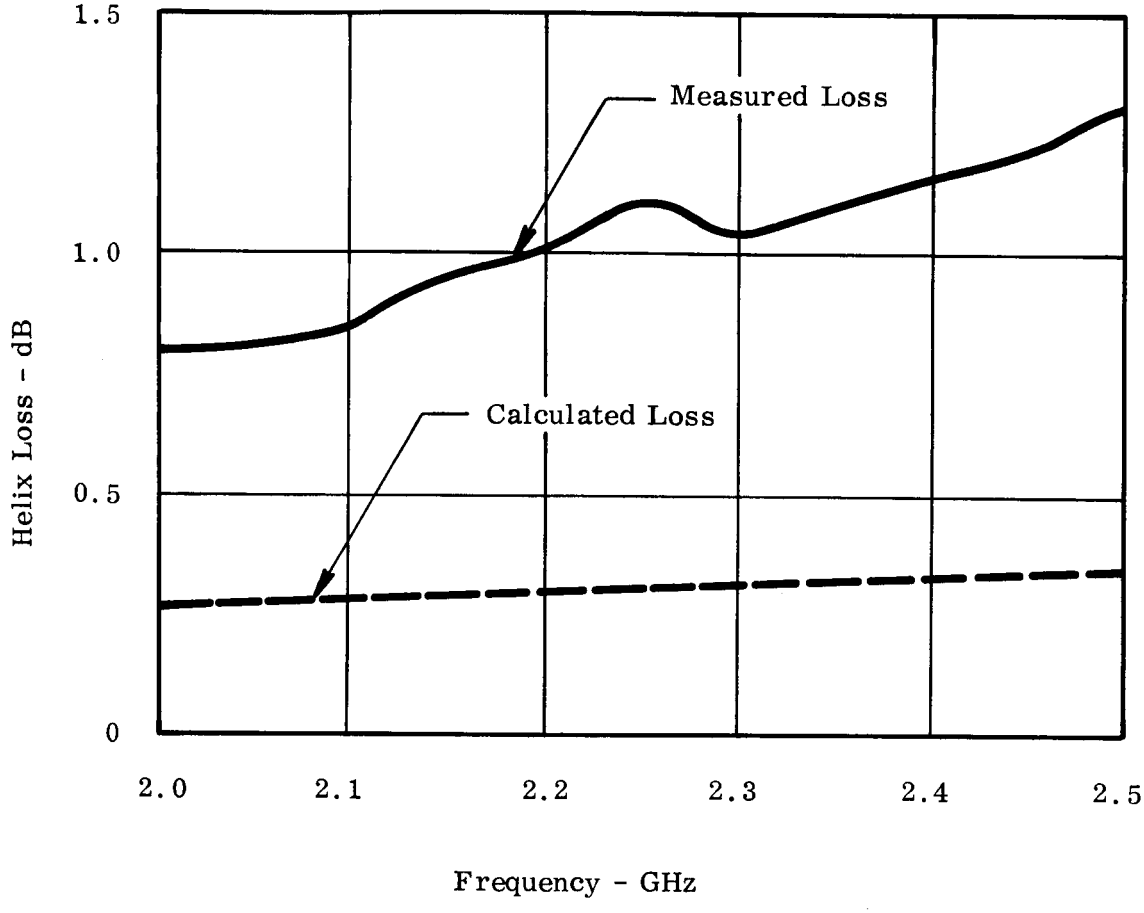

Fig. 7 - Plot of measured loss and loss which should have been obtained on attenuator-less helix section of WJ-395 S/N 5.

electrons. These secondary electrons are accelerated across the sever gap in a direction depending upon the direction of the electric field gradient. In most cases this is in the direction of the second-stage helix. This large value of current, which can exceed 10 mA with a voltage difference of 100 to 200 volts, confused the evaluation of the electron beam focusing by adding to the intercepted current on one helix and subtracting current from the other.

Performance of the Tube

In general, this tube had lower beam efficiency performance and higher helix current interception than would be expected. Fig. 8 shows a plot of power output, saturation gain and beam efficiency vs. helix voltage at a beam current of 115 mA for Helix Section No. 1 alone. These conditions should have led to a beam efficiency greater than 30 percent. As a result of the lower efficiency, the power output reached only 66 watts which is just two-thirds of the expected 100 watts. Fig. 9 shows a power transfer curve.

Two helix performance is shown in Fig. 10. This corresponds to the case where the voltages of the two helices are the same or nearly the same. Maximum power output of helix No. 1 and helix No. 2 is the same for a given set of conditions. Thus efficiency is identical. It takes more input drive power to reach the peak of helix No. 1 alone. The small signal gain of the tube when observed from the output of helix No. 2 has a more normal characteristic and does not show so much evidence of the gain expansion which is typical of large overvoltage operation. This is accounted for by the output section which is operating much nearer to synchronism and therefore provides about 7 additional dB of small signal gain. A tube operating in this manner is almost identical to "positive taper" operation. The data for the helix No. 1 output curves were not carried to higher values of power input than shown because of the large helix current interception which resulted in this region.

It was found that the maximum beam efficiency occurred when the voltages of helices No. 1 and No. 2 were the same value. This was not expected, and does not correspond to the data measured by Niclas and Gerchberg. Fig. 11 shows two sets of curves measured with a difference voltage of approximately 40 volts between helices. Comparing the output of helix No. 2 at 2740 volts in Fig. 10 to the output of helix No. 2 at 2790 volts in Fig. 11, the beam efficiency decreases slightly from 14.6 to 14.3 percent. In these cases, the

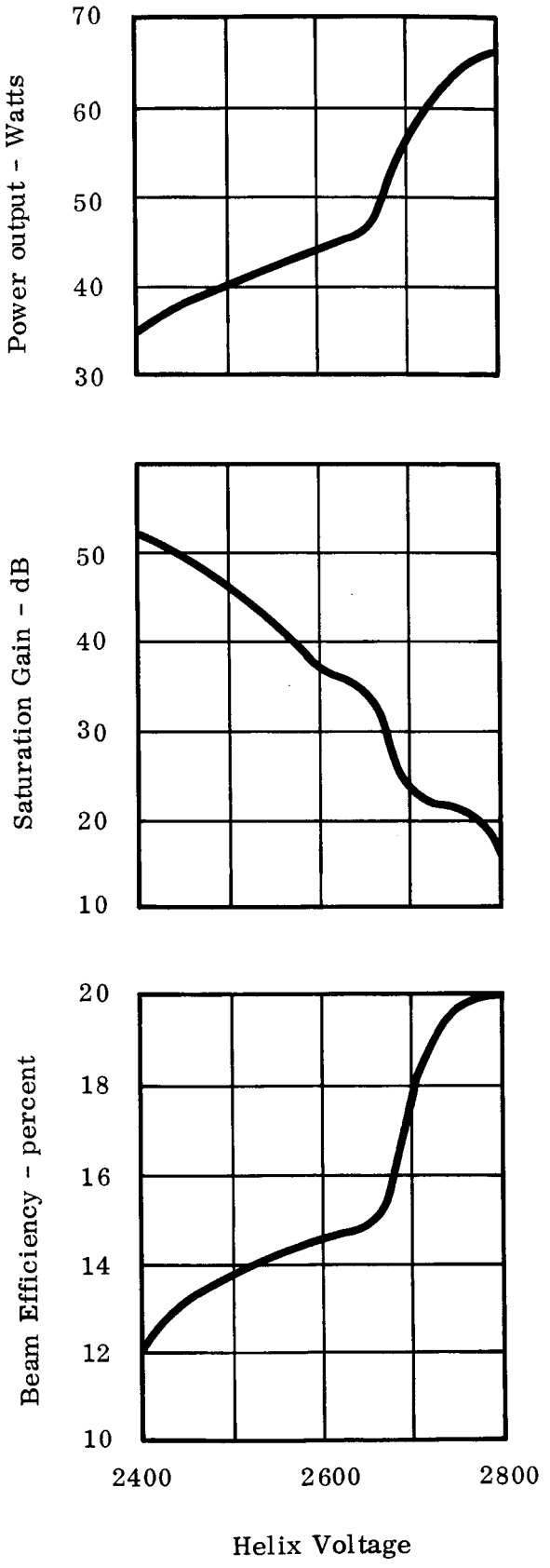

Fig. 8 - Power output, saturation gain, and beam efficiency of WJ-395 S/N 5, Two-helix tube. First stage performance only. Beam Current = 115 mA, Frequency = 2.3 GHz.

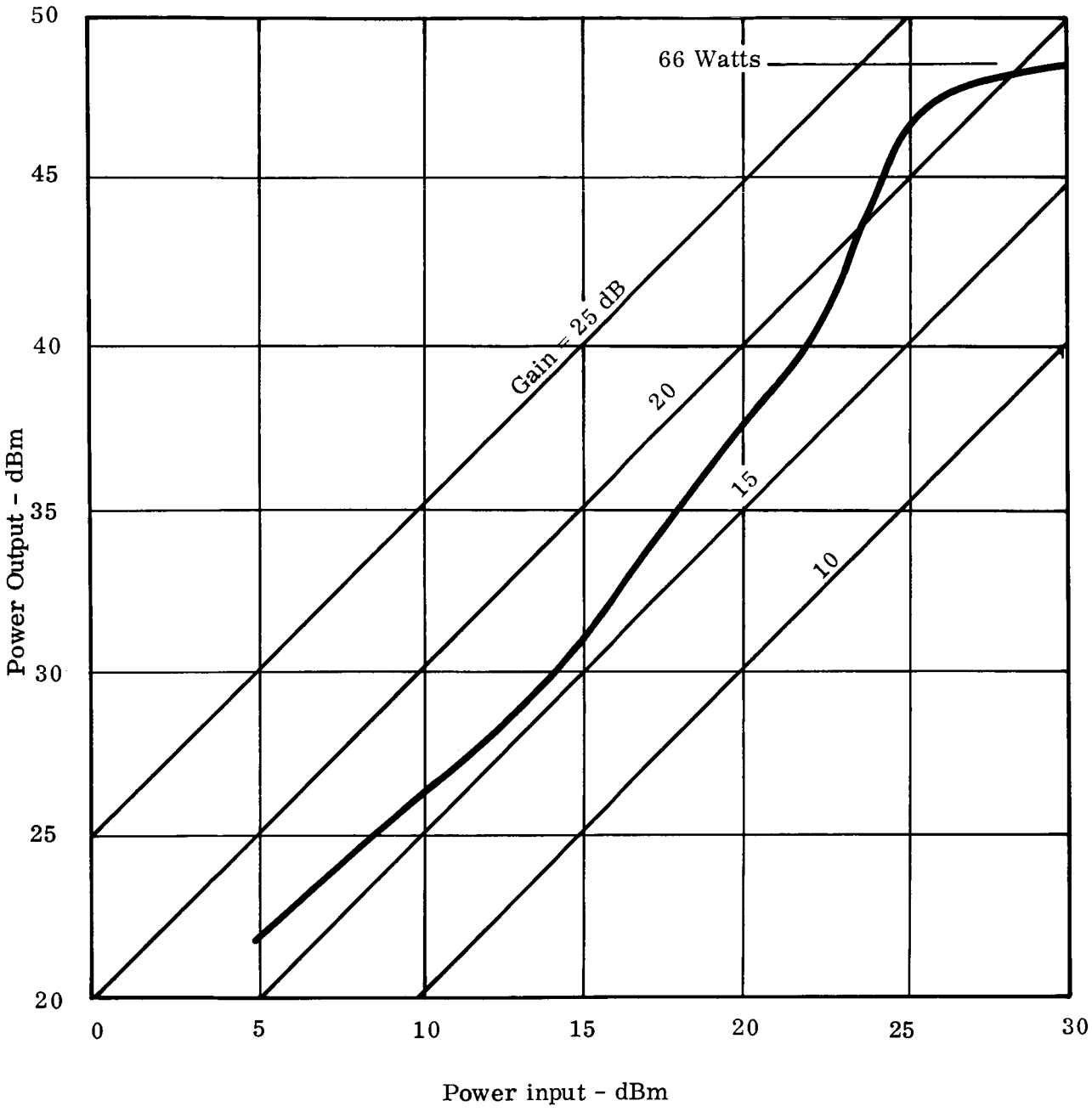

Fig. 9 - Power output vs. power input for WJ-395 S/N 5, two-helix tube, first-stage helix performance only. Helix voltage = 2790 V, Beam Current = 115 mA, Frequency = 2.3 GHz.

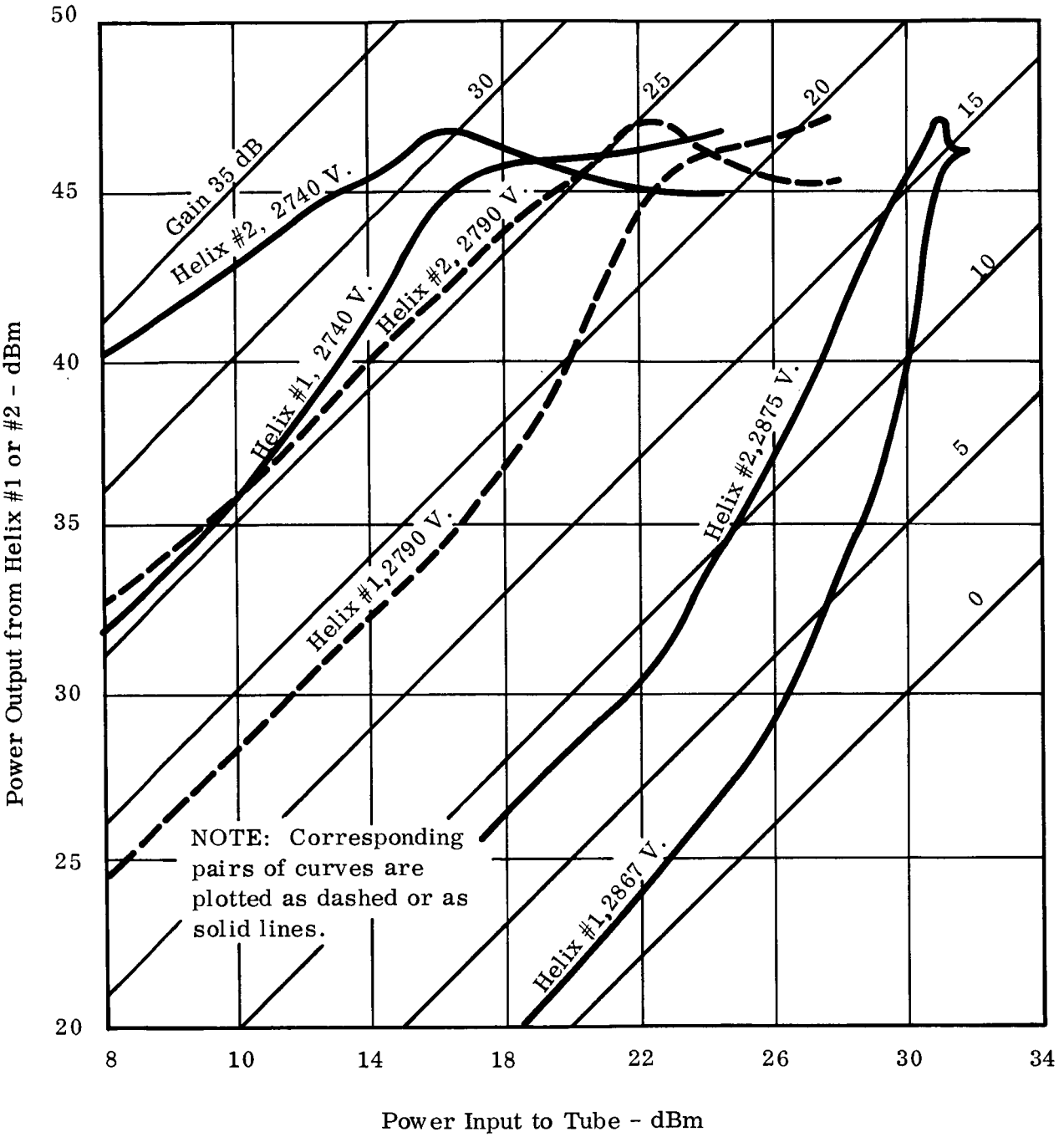

Fig. 10 - Power transfer curves for two-helix tube, WJ-395 S/N 5. Curves are in pairs showing power output from Helix #1 and Helix #2. Conditions are for helix voltages which are the same or nearly the same. Beam current = 120 mA. Frequency = 2.3 GHz

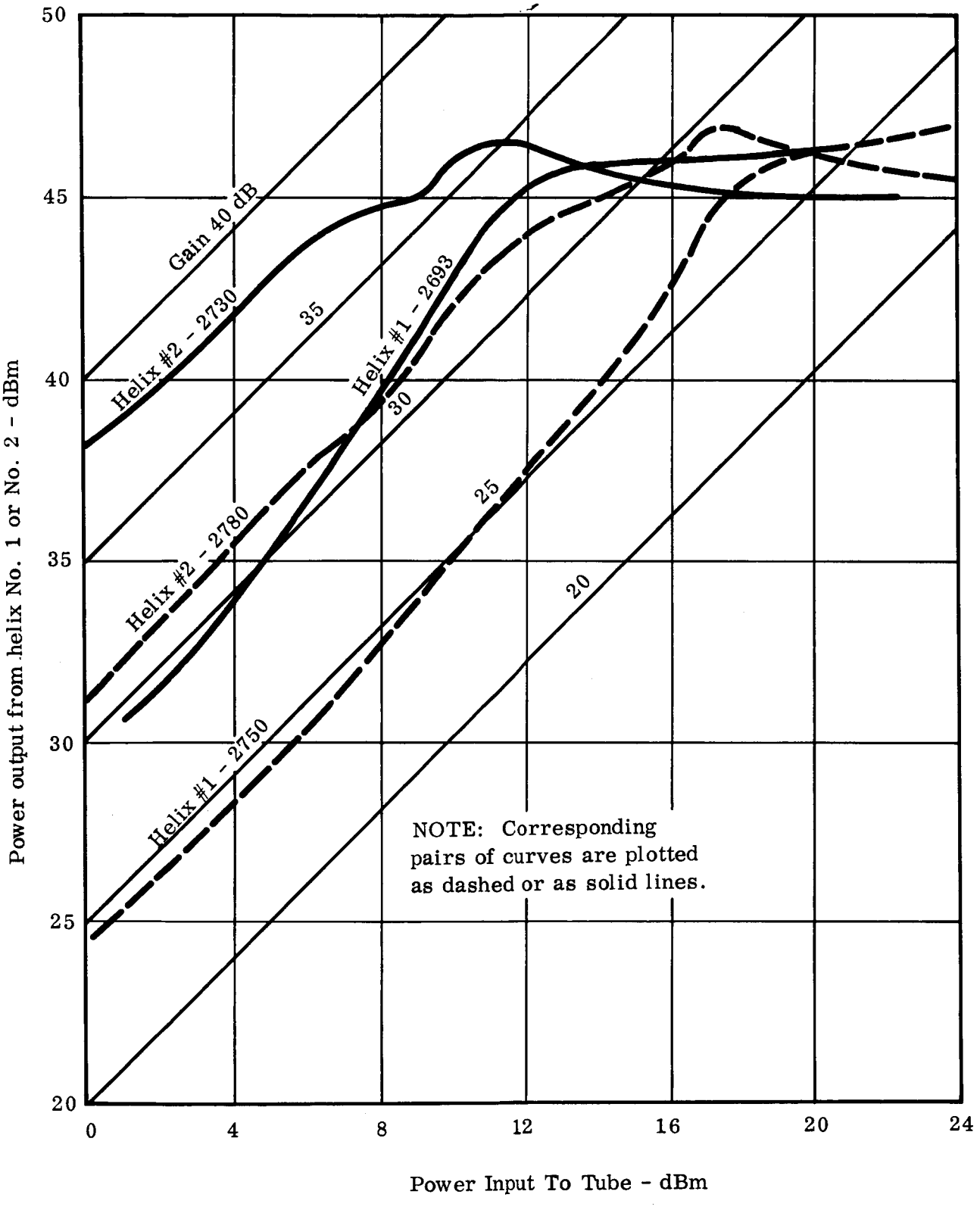

Fig. 11 - Power transfer curves for two-helix tube, WJ-395 S/N 5. Curves are similar to Fig. 10 except that helix No. 2 has approximately 40 volts more than helix No. 1. Beam Current = 120 mA. Frequency = 2.3 GHz.

helix No. 1 was at almost the same voltage. Tests showed that as the voltage difference was made larger, the efficiency decreased and secondary electron current rose to very large values.

The results of the tests did not prove or disprove the value of the two helix tube as an efficiency enhancement device. This resulted from the poor power and efficiency results which have been attributed to the lossy helix structure. Now that a two-helix tube has been built and tested, certain disadvantages can be seen. These are discussed in the following section.

Discussion of Disadvantages of the Two-Helix Approach

1. Construction Complication

The construction of the two-helix tube is difficult. It took more than twice the effort to construct it compared to a comparable single-helix tube. The configuration of the second sever (see Fig. 5) is not ideal. There is almost no room to mount the impedance reducers at the helix to coax transitions and fasten them inside of the tube barrel because of the restricted space. In addition, the body braze which can be simply accomplished at the first sever with a bell-jar radiation braze because of the low heat drain away from this joint, becomes very difficult at the second sever. This is due to the fact that there are rigid pole piece and outer conductor assemblies on either side of the second sever. These drain the heat away from the braze joint and require a much longer application of heat to accomplish this braze. Since the helices are already mounted in the body assemblies at this time, it subjects them to excessive temperature and the possibility of evaporation of lossy coatings onto the helix support rods. This could ultimately be corrected by redesigning this joint to be closed with a heli-arc weld. The body and sever parts would have to be redesigned in this area. The technique of performing the weld would have to be worked out with practice pieces and perhaps special electrodes because the accessibility of the joint is poor because of the window mounts which overlap the joint.

2. Drift Length of the Sever

The second sever occurs in the large signal region of the electron beam interaction. Since there is a practical minimum mechanical distance of two magnet cells from the end of the helix No. 1 to the beginning of helix No. 2 (0.390 inches as shown in Fig. 5), the electron beam must drift in a field free region for this distance. This is not good practice in the large signal region because appreciable space charge forces exist in the beam at this point. These can cause debunching in the absence of a strong rf electric field on the helix and quite possibly will effect efficiency performance. Even with the same physical length as in the Niclas-Gerchberg two-helix tube, it will be electrically twice as long because of the operating frequency which is slightly more than twice as high. No experiments have been performed to show how critical this drift length is on efficiency performance.

3. Secondary Electron Emission at the Second Sever

This problem was described earlier and confuses the picture of beam transmission. The three current components due to (1) primary electron interception, (2) secondary electron interception and, (3) returned electrons from the depressed collector are indistinguishable. The dissipation due to the secondary electron component is much lower because the electrons are accelerated only across the voltage difference between helices. It is hard to judge how much electron interception can be tolerated under these conditions before damage is done to the helix. It further confuses the meter readings because the helix which emits the secondaries has that current component subtracted from its primary interception component and can in some cases read negative because the secondary current is greater than the primary.

4. Impedance Matching of Helix No. 2

Matching of the short, low-loss, unattenuated helix No. 2 to the external transmission line is a difficult task because we have not been able to find a satisfactory way to adequately terminate this short section of helix. Since it cannot be properly terminated, standard reflection coefficient or VSWR measurements made looking into the helix through the external transmission line do not give a

simple picture of the discontinuity between the helix and transmission line. In the normal helix with center attenuation, the helix is so well terminated that the discontinuity between the helix and the transmission line represents the only source of reflection. In that case it is simple to adjust the transition for minimum reflection. In the case of the short low-loss section of helix, it is necessary to attempt to terminate the helix with an insertable termination. We were not able to make one with a sufficiently low reflection coefficient of its own and enough attenuation to isolate the discontinuity at the opposite end of the helix. Any matching adjustments cancelled out some of the termination reflection and some of the discontinuity component from the opposite end of the helix as well as the discontinuity between the transmission line and the helix. As a result, the effective reflection coefficient of the transmission line to helix transition is an unknown. This is a problem at both ends of this short helix section.

5. Non-uniform Period in PPM Stack

A factor which may have contributed to the poor focusing under rf drive conditions was the presence of three magnet cells in the large signal section at the second sever which were a different period than the surrounding stack. This is shown in Fig. 5. Because of the wider magnet cell width required for the stripline outer conductors and for the second sever, it was necessary to increase the magnet length in the three cells comprising the sever and those on either side of it. There may be in addition to the change in period, additional transverse magnetic fields due to the fact that the magnets in the stripline cells are not continuous circles but have a gap to allow the stripline outer conductor to pass radially outward. These cells have been programmed to have the same peak field as the rest of the magnet stack, so there is not a discontinuity in the peak value of the field.

6. Ion Trapping

One problem which arises as a direct result of the two helix operation with the helix No. 2 at a higher potential than Helix No. 1 is the trapping of ions in the helix No. 1 region. The anode which is at a higher potential than the helix acts as an ion block to keep the ions from draining into the cathode for long life reasons. With the helix

No. 2 at a higher potential than helix No. 1, a potential well is formed. Ions which are created by collisions between electrons of the beam and neutral gas molecules in the helix No. 1 region, do not have enough energy to climb the potential barriers and build up to form an appreciable ion space charge in this region. They tend to neutralize the electron space charge of the beam thereby shrink the beam diameter and form an ion cloud on the tube axis. The rf performance of the tube changes in the presence of the trapped ions because of the change in the beam diameter. The presence of the ions also will induce ion noise modulation on any signals which the tube is amplifying. The magnitude of this effect has not been measured in this tube, but has been the subject of extensive studies elsewhere and has been shown to result in very real problems.

As of the present writing, no satisfactory means of draining this ion beam in this configuration has been devised. Because of the magnetic containment of the beam, the ions cannot be drained radially through the beam to an electrode placed in the tube at the proper location and potential.

7. Extra Voltage Requirements

A further disadvantage of the two helix structure is the requirement of an extra voltage for helix No. 2. This is a complication to the power supply and will in general lead to a slightly lower power supply efficiency because of the added transformer windings, rectifiers and filters required.

This added voltage requirement means that the helix No. 2 must operate at a voltage difference with respect to the body of the tube. There is always the possibility of voltage breakdown or leakage currents building up with time. This latter might occur due to ion deposition of material on the helix rods during the course of life of the tube. This problem does not exist on a tube in which the helix operates at body potential.

8. External DC Blocks

The requirement for the helix No. 2 to operate at a potential difference with respect to the body also requires a means for isolating

the center conductor of the external transmission line from this helix. This then requires a dc block at both windows capable of withstanding the voltage difference. This must be done in such a way that a very high reliability of performance is assured under the full environmental range of conditions including performance through critical pressure. A failure of this dc block could render the tube inoperative. In addition, one of the blocks must be designed to also apply the voltage to the helix No. 2 without interfering with the rf properties of the block. Commercial versions of such a device are available for use in laboratory tests. It is bulky and unsuitable for use in space systems. A specific device would have to be developed capable of meeting all the requirements.

Discussion of Possible Advantages of the Two-Helix Approach

There is now no demonstrated advantage "efficiency-wise" of the two helix tube since both devices have shown in excess of 40 percent beam efficiency and have shown efficiencies with depressed collector of 51 percent. The advantage of the simplicity of the single helix tube both from the construction and the power supply standpoint is easily recognized.

There is a possible advantage of the two helix tube with the velocity jump between helices, although this has not been demonstrated at the present time. This is related to the distribution of the slow electrons in the spent beam as it enters the collector. If the slowest electrons in the bunch can be confined more closely to the average beam velocity, then the collector can be depressed to a lower potential and greater overall efficiency can be obtained.

A deamplification of the velocity spread of the electrons occurs in the velocity jump between helices due to the potential increase. The entrance conditions of the electron velocity distribution into the helix No. 2 is better than would occur into a positive taper section of a unipotential helix. Adequate tests on a two helix tube, operating at high efficiency, have not been performed with a collector specifically designed for depressed operation. The only depressed collector measurements on a two helix tube have been performed with a beam velocity and current analyzer which did not have a beam collection system designed for depressed operation.

Conclusions on Tube WJ-395 S/N 5

The results of the tests on this tube were certainly not conclusive since efficiency results were masked by loss problems and also to some extent by focusing. It became clear that the construction of this type of tube would always be considerably more difficult. To build a successful version now would require special effort to work out certain constructional problems previously discussed. Since equivalent performance has now been demonstrated with single-helix, unipotential helix tubes, there is a very strong reason to proceed in this latter direction. We propose not to proceed with any further two helix work on this program since it is felt that this is the least desirable solution to the problem and would constitute the least efficient use of project funds. It is proposed that further work on the two helix type tube be followed on exploratory or research programs.

WJ-395 S/N 6

Design Basis

The WJ-395 S/N 6 is a tube scaled from Tube S/N 3 of the company-sponsored research program. S/N 3 had demonstrated a beam efficiency of 41 percent and an overall efficiency of 51 percent at a power level of 20 watts and a frequency of 1.2 GHz. S/N 3 had a beam perveance design value of 0.80×10^{-6} which is the same as the design perveance of WJ-395 S/N 5.

Fig. 12 shows a photograph of a three-dimensional model of the efficiency characteristics of S/N 3 plotted on the helix voltage-beam current plane. It is seen how the efficiency sharply rises as both helix voltage and beam current are increased in the proper combination. Fig. 13 is a photograph of a similar three-dimensional model for saturation gain.

The design of WJ-395 S/N 6 was based upon the above tube design with some slight modifications to allow for certain practical

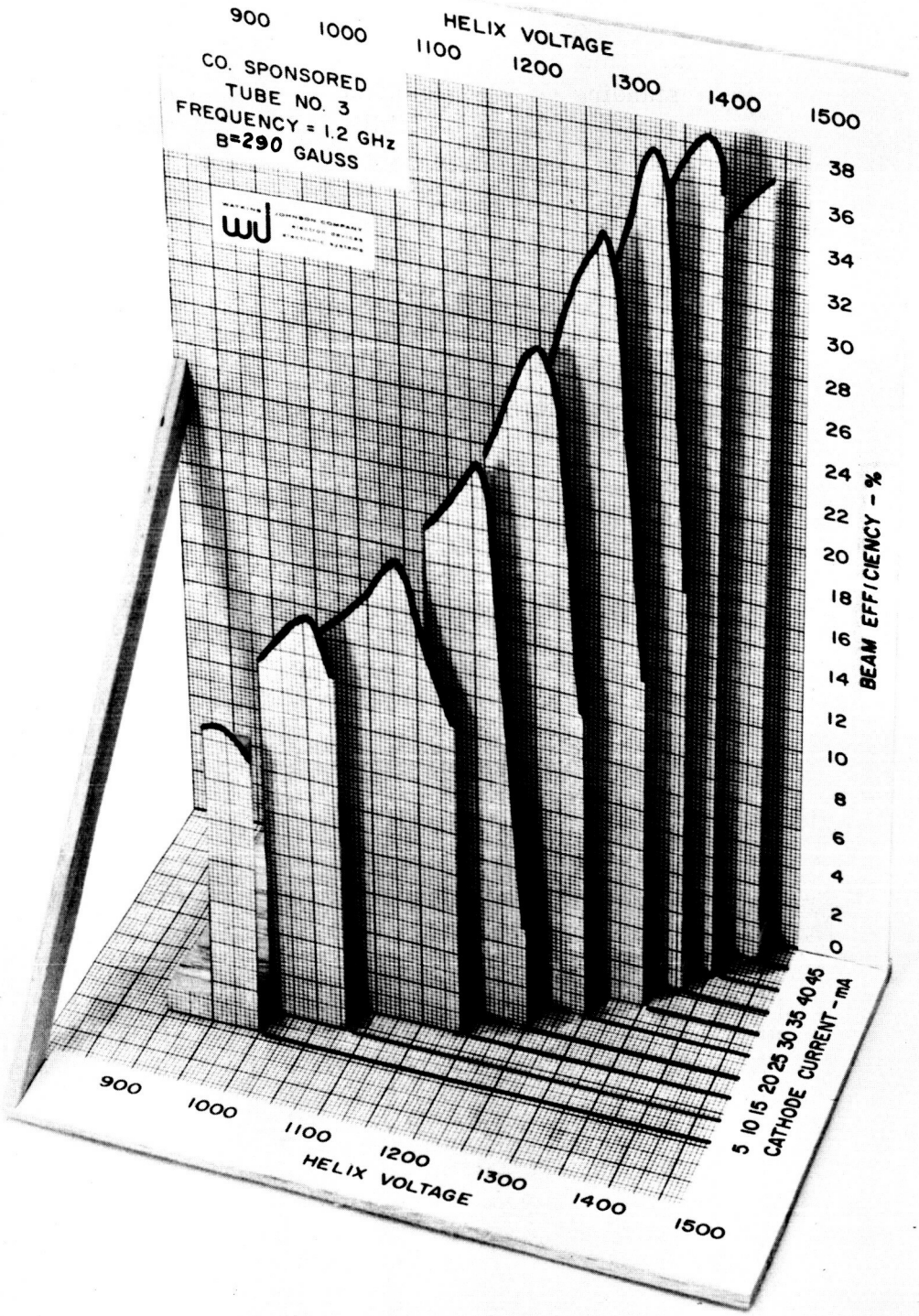

3463

Fig. 12 - Photograph of three-dimensional model showing efficiency plotted on the helix voltage-beam current plane of company-sponsored tube S/N 3.

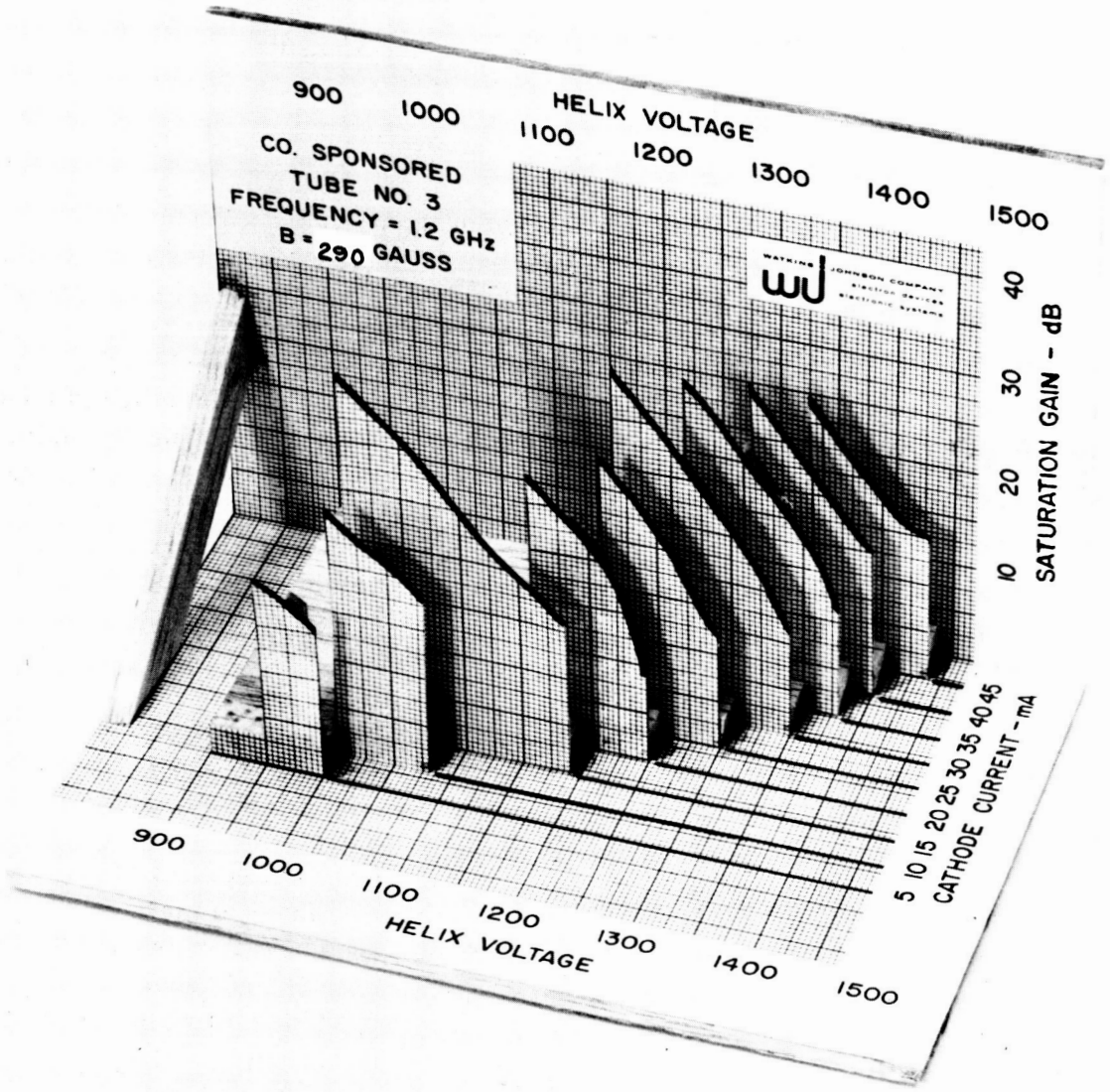

3463-1

Fig. 13 - Photograph of three-dimensional model showing saturation gain plotted on the helix voltage-beam current plane of company-sponsored tube S/N 3.

differences between the tubes. The following parameters were used as the basis for scaling:

Power output = 100 watts
Beam Efficiency = 35 percent
Perveance = 0.80×10^{-6}
$\gamma a = 1.2$

There are certain differences in the designs. The exact effect of these differences is unknown. One of these is the ratio of the barrel inside diameter to mean helix diameter. It is 1.85 on the company-sponsored tube and 1.65 on the WJ-395. This decreased the helix impedance because of the change in dielectric loading and wall loading. The company-sponsored tube is solenoid focused while the WJ-395 is PPM focused. The attenuator drift length, measured in reduced plasma wavelengths, is only slightly longer on the WJ-395 because of effort made to reduce its length by making it a continuous, non-severed attenuator. Fig. 14 shows helix, magnet and attenuator configuration for the tube.

New Collector Design

The major mechanical change on this tube was the use of the new collector design. A photograph of an exploded view of the collector is shown in Fig. 15.

The beam current is collected both in the cylindrical barrel of the collector and in a conical hole machined into the main copper piece seen at the right of the photograph. The heat flow path is downward into the base of the collector. This path is very short and has a large cross-section of copper which provides a low temperature drop. The collector is insulated from the capsule by a beryllium oxide disc not shown in the photograph. The heat transfer contact is maintained through the beryllia disc by pressure onto an inside flat surface of the capsule. Fig. 16 shows a snout end view of the collector without its steel jacket. Fig. 17 shows the collector with the steel jacket and cover in place. The purpose of the jacket and cover is to provide a means of applying pressure to the collector to force it tightly against the beryllia disc. Because the annealed copper of the collector is so soft, pressure could not be applied to the top of the

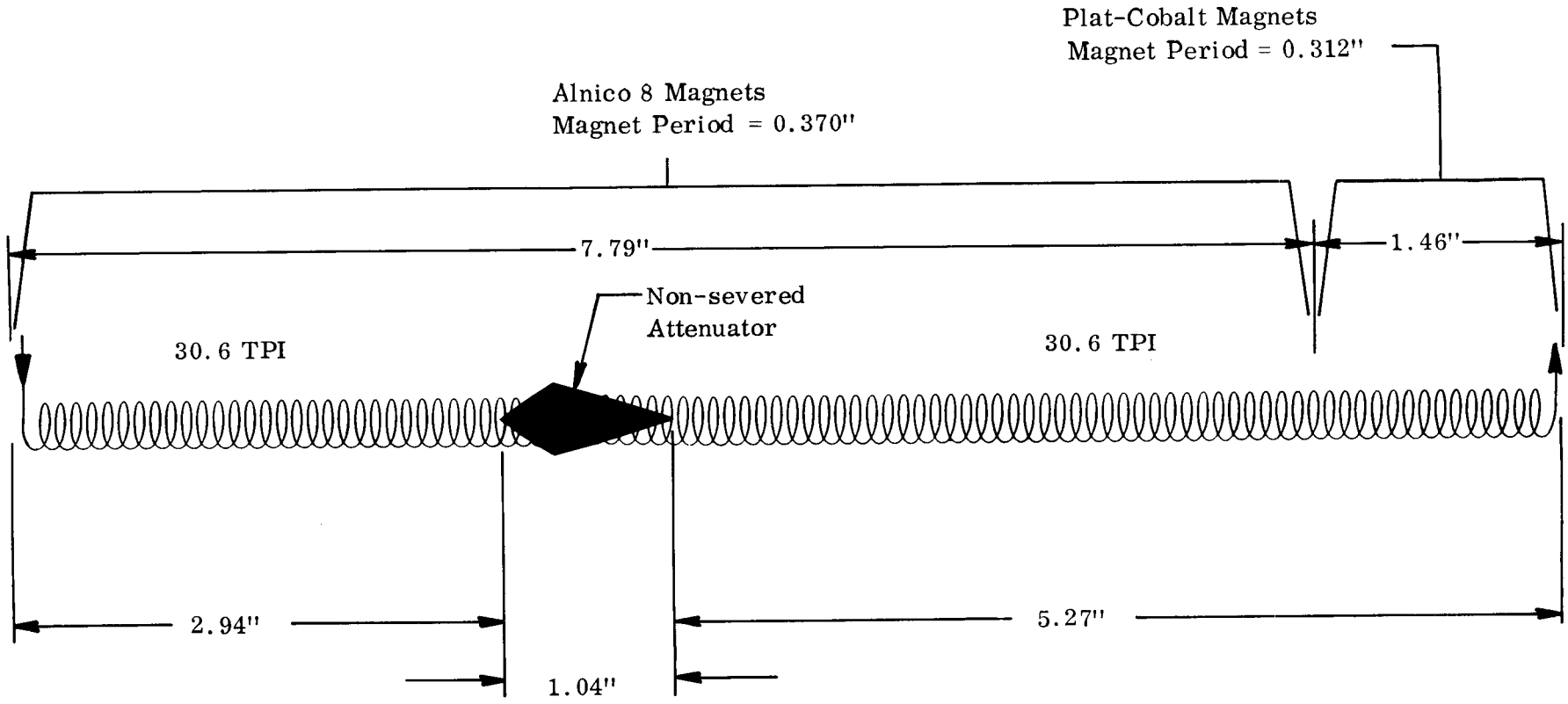

Fig. 14 - Helix, Magnet and Attenuator Configuration of WJ-395 S/N 6.

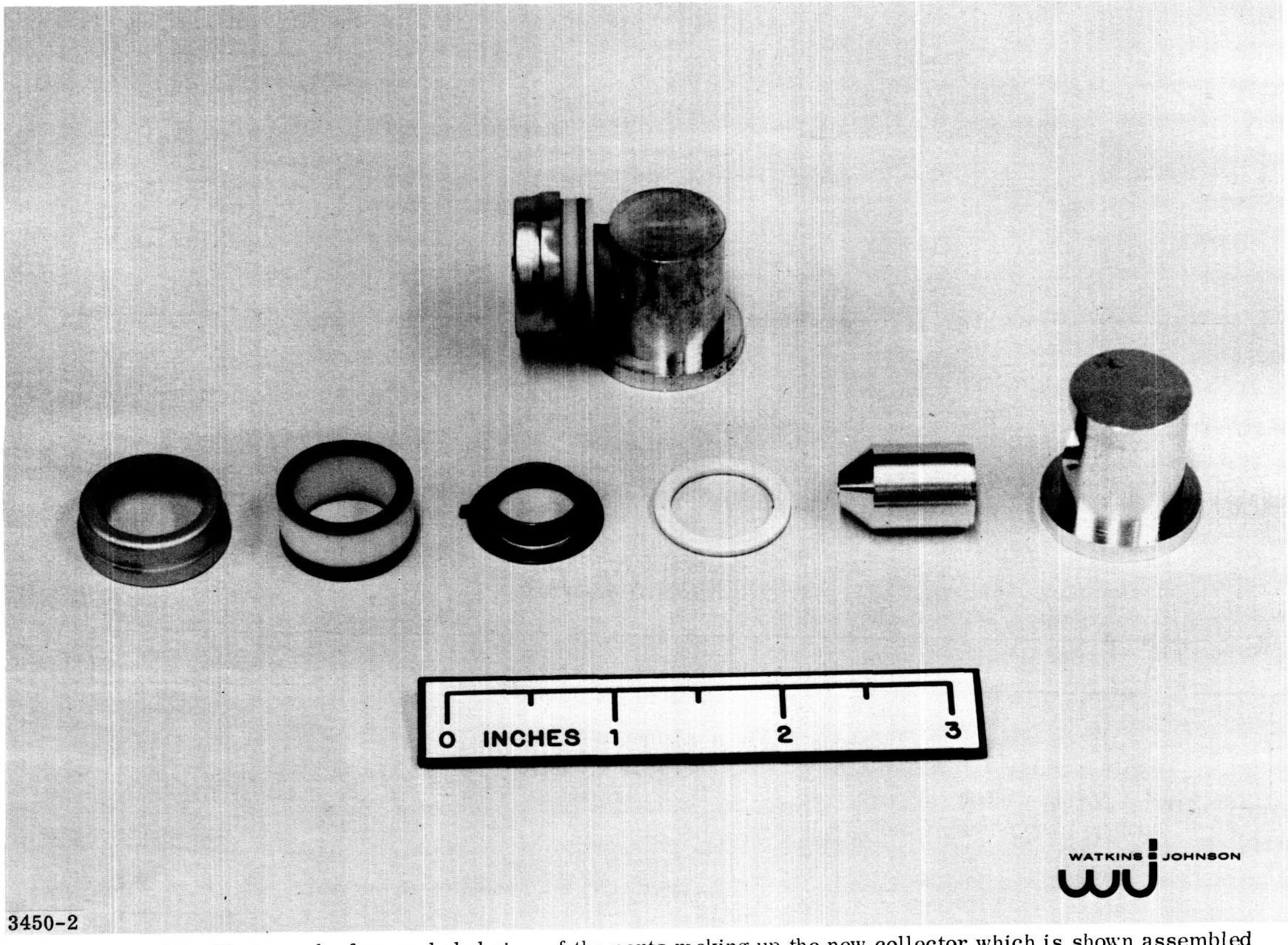

Fig. 15 - Photograph of an exploded view of the parts making up the new collector which is shown assembled in the background.

Fig. 16 - Photograph of a snout end view of the collector without the steel jacket.

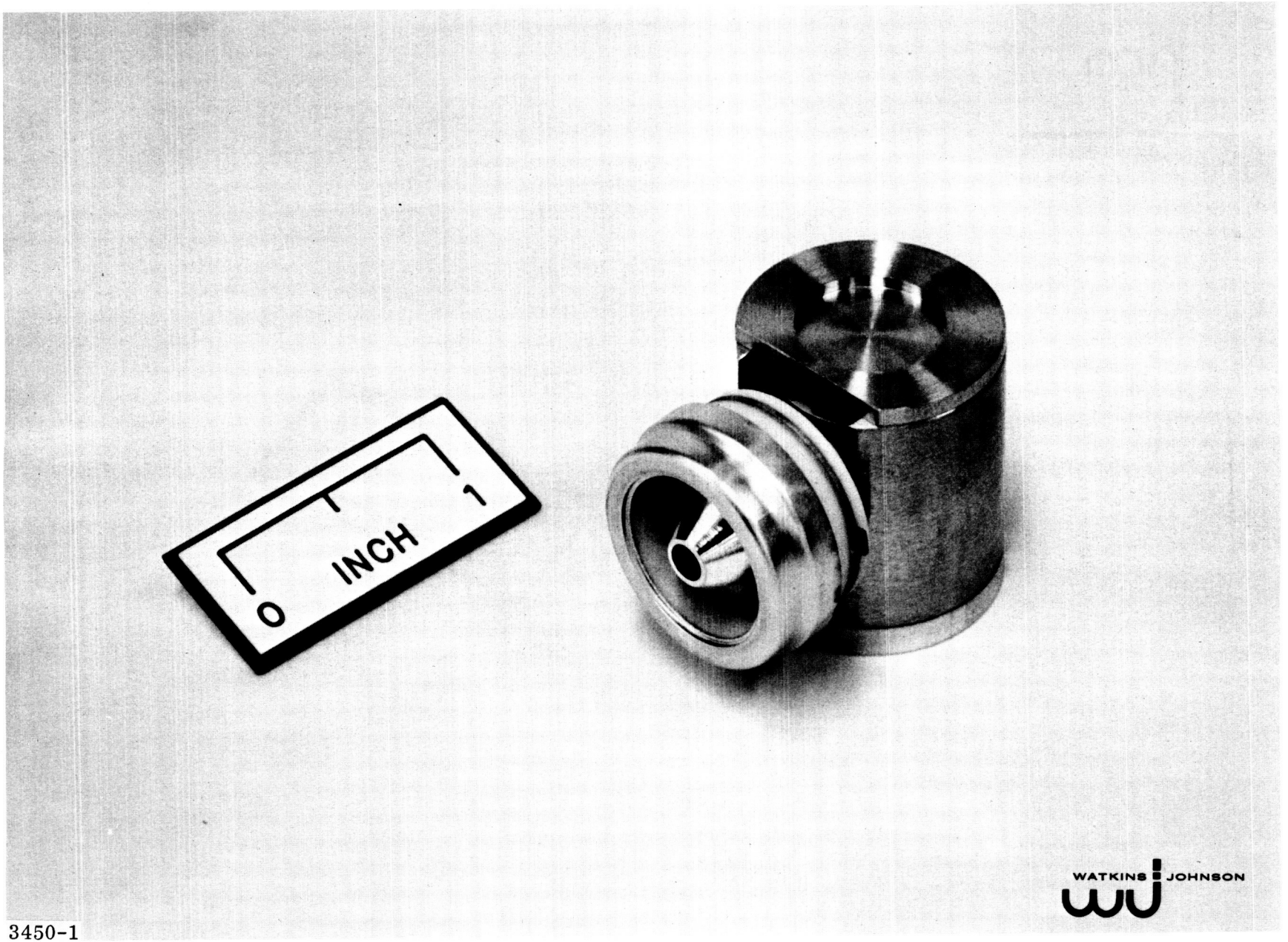

Fig. 17 - Photograph of the collector with steel jacket and cover in place pressing on the lower lip.

collector without deforming it. Pressure is applied by a screw from the top of the capsule through a thick aluminum oxide disc insulator which sits in the recess of the steel cover. The force is then transmitted through the jacket to the lower lip of the collector which forces the copper tightly onto the beryllia disc. No pressure is applied to the upper portions of the collector. The interfaces between the copper and beryllia, and the beryllia and the bottom of the capsule are coated with a thin layer of heat transfer compound. The final material has not been chosen yet.

Calculations show that with 300 watts of power flowing into the collector, the maximum temperature drop from the collector hot spot to the capsule should be about 60^{o} C. This should be compared with Table II of quarterly Report No. 3 for the old style collector. With heat sink temperatures of 75^{o}C as required in the specifications, the collector hot spot will be less than 150^{o}C which is well within the ratings of the potting materials.

On WJ-395 S/N 6, at conditions corresponding to 87 watts of RF output but with no drive, the top of the collector measured 82^{o}C, the bottom of the collector at the beryllia disc was 52^{o}C and the baseplate heat sink was 20^{o}C. This represents a total drop from the heat sink to the hot spot at the top of the collector of only 62^{o}C under no drive conditions.

Under saturated output of 87 watts, the top of the collector was 51^{o}C, the bottom of the collector at the beryllia disc was 31^{o}C and the baseplate heat sink was 16^{o}C. This is a temperature drop from heat sink to hot spot of 35^{o}C.

These tests were made with silicone grease at the interfaces. At a later time, tests will be made to try various materials as heat transfer compounds.

A photograph of WJ-395 S/N 6 mounted on its laboratory baseplate is shown in Fig. 18. The collector is pressed down onto the beryllia disc and baseplate with the pressure screw in the same way that it will be done in the actual capsule. The tube can be set up for tests very quickly with this system.

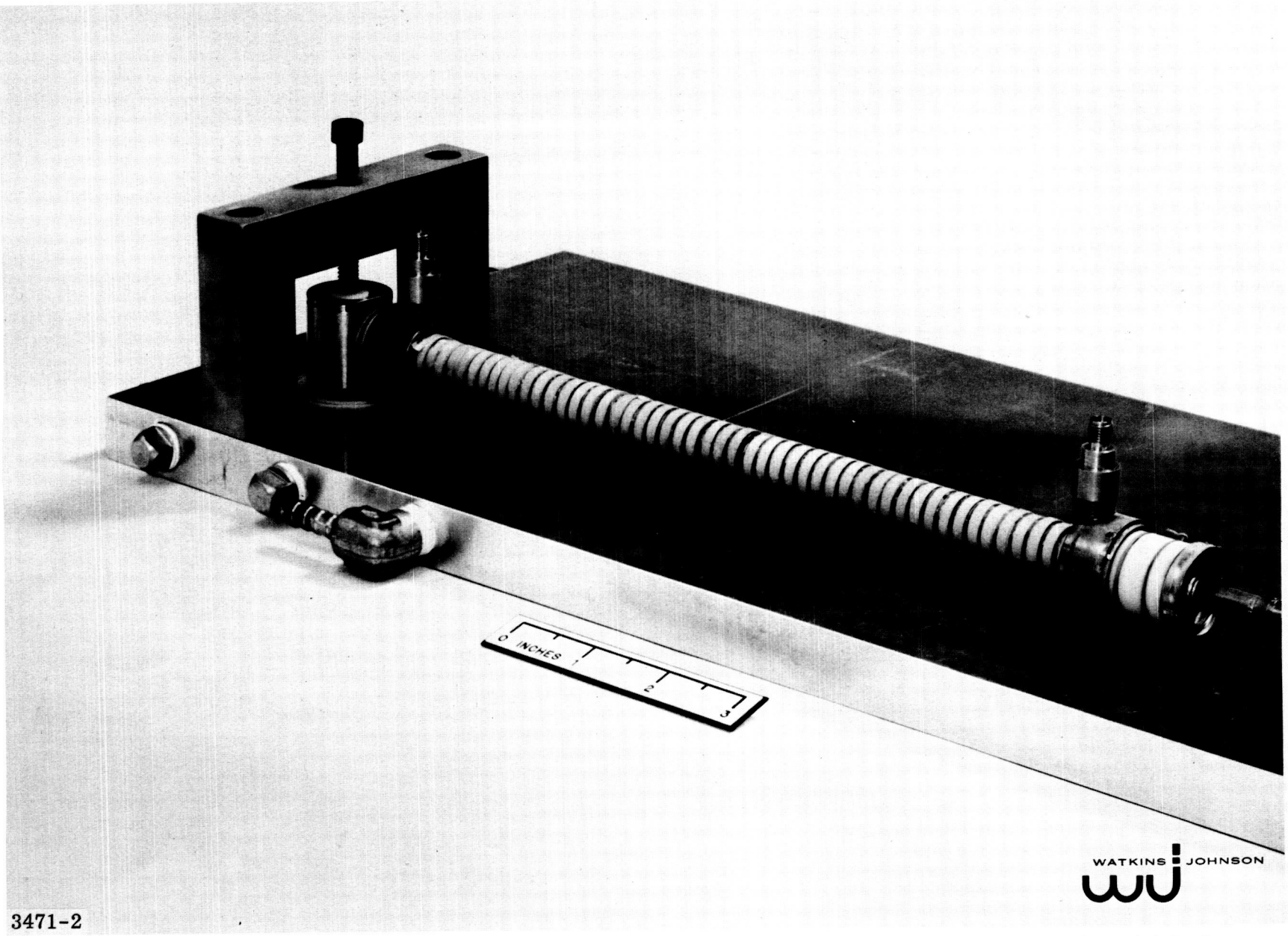

Fig. 18 - Photograph of WJ-395 S/N 6 mounted on its laboratory baseplate for experimental tests.

Performance

The standard plot of power output, saturation gain and beam efficiency of WJ-395 S/N 6 measured at 2.3 GHz is shown in Fig. 19. It is seen that 36 percent beam efficiency is reached at 100 watts and is still 34 percent at the 66 watt level. This is the highest beam efficiency observed on the program to date. The fact that the beam efficiency is close at these two different power levels implies that the overall efficiency should also be close.

Power output, saturation gain and overall efficiency (including heater) is plotted vs frequency in Fig. 20. At 66 watts, overall efficiency of 45.2 percent and at 100 watts, overall efficiency of 44.1 percent was measured. The efficiency exceeds 40 percent over a 300 MHz bandwidth at the 100 watt level, and over a 400 MHz bandwidth at the 66 watt level.

Fig. 21 shows a plot of power output vs power input for the tube operating at the two different power levels. The operating voltages and beam current have been appropriately shifted for the two cases. It is seen that the tube has very low small signal gain and has the very rapid rate of rise of power output with drive as the saturation region is approached. This is typical of highly overvoltaged operation. The region of interest really is in the neighborhood of saturation since this is where the high efficiency occurs. This is shown in detail in the plots of Fig. 22. The upper plot is the case of fixed beam current (fixed anode voltage) where transfer curves are plotted for three values of helix voltage. This represents ±0.5 percent change in helix voltage. The lower plot is more typical of performance which would be obtained in a space type of power supply where the helix and anode would vary proportionately together. In this case, where beam current and helix voltage vary together, the spread of the curves is less for the ±0.5 percent voltage change. At a fixed set of voltages, a drive power variation of 1.6 dB will give a decrease in power output of 0.5 dB from saturation. This is equivalent to saying that the efficiency will remain above 40 percent for a drive power variation of 1.6 dB under fixed voltage conditions. The curves also show that efficiency will stay above 40 percent for a power supply variation of about 0.6 percent at fixed drive. A broadening of the top of the saturation curve is one of the goals of the subsequent development tubes.

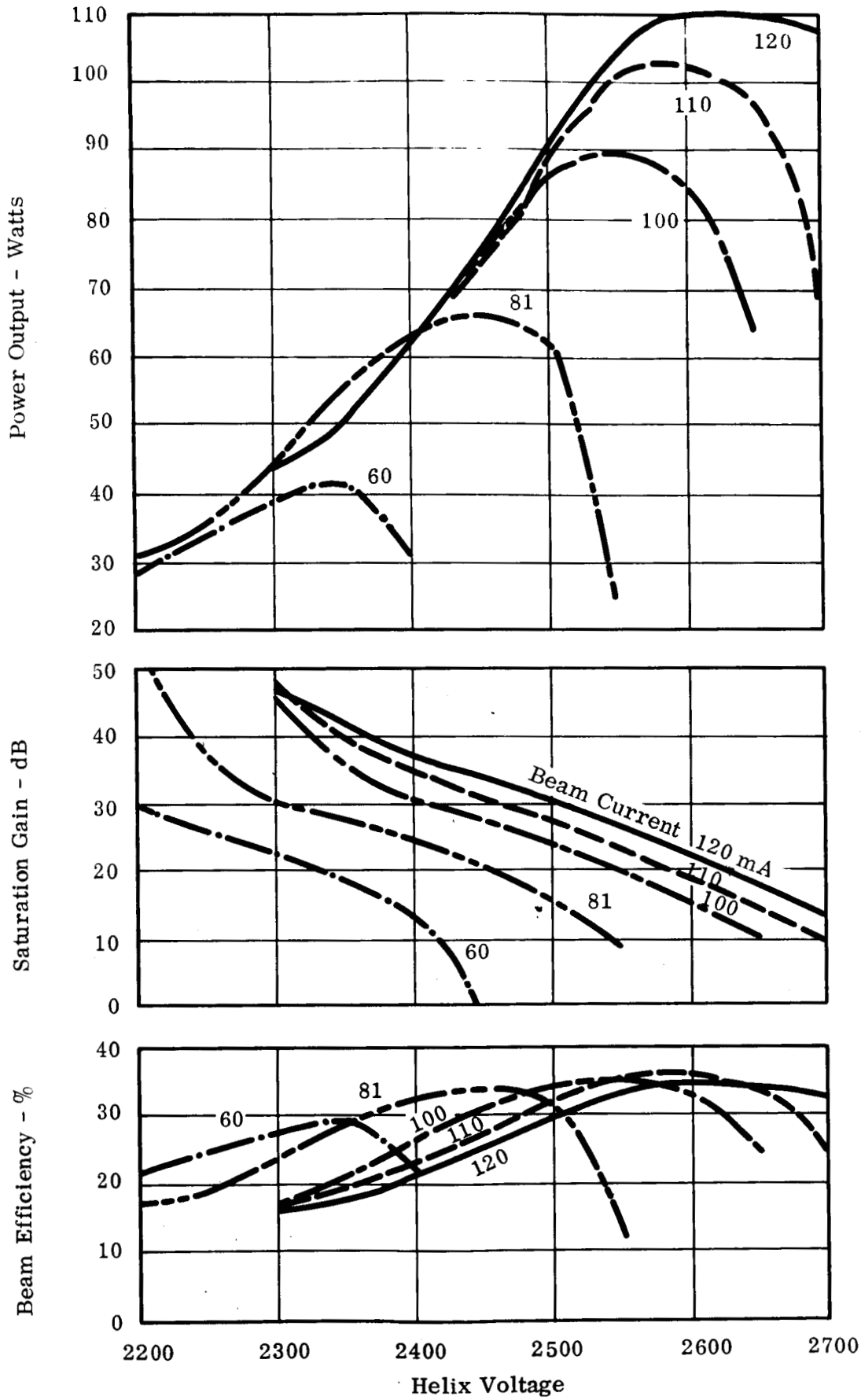

Fig. 19 - Plot of power output, saturation gain and beam efficiency vs helix voltage with beam current as a parameter of Tube WJ-395 No. 6. Frequency is 2.3 GHz.

17372

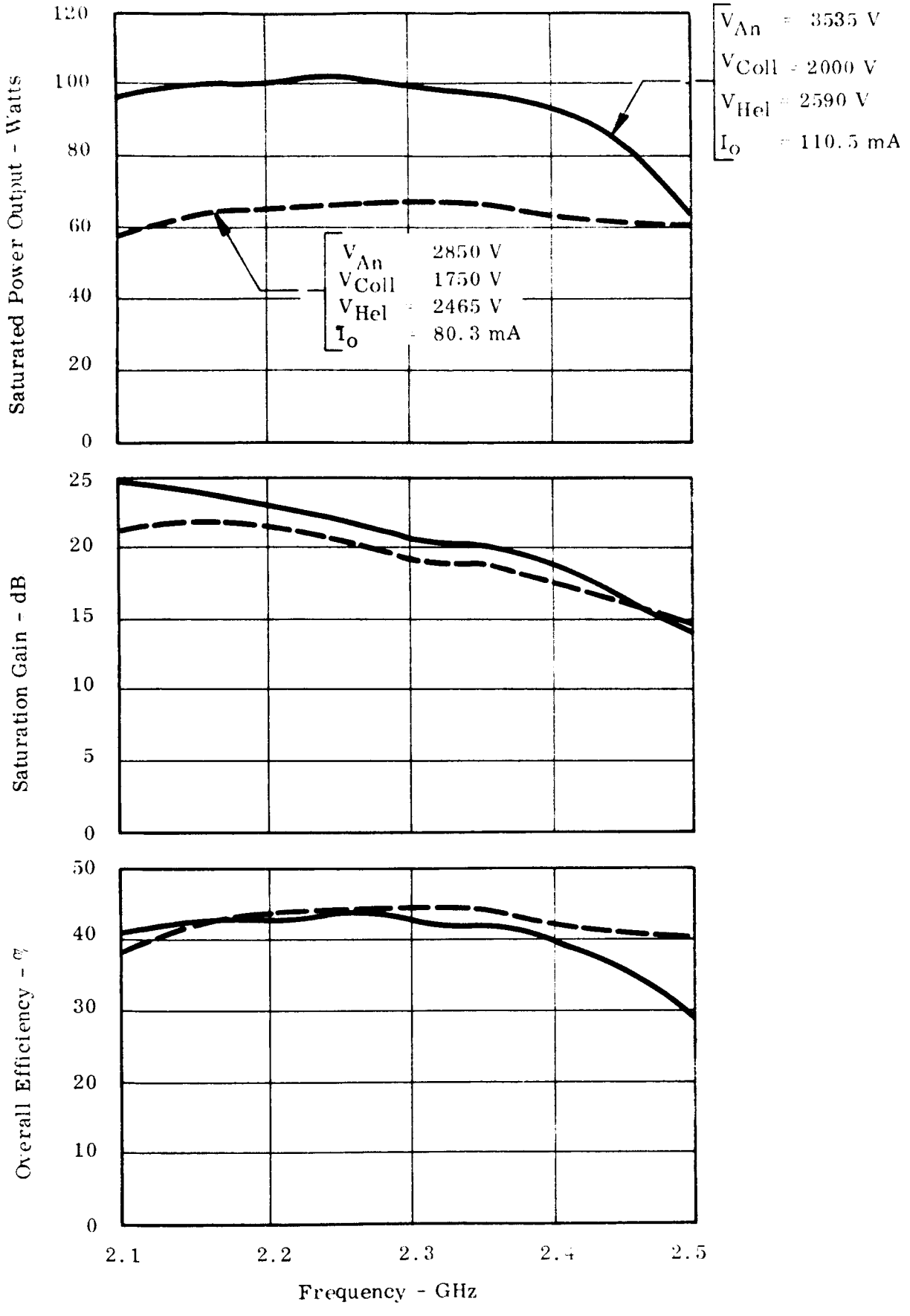

Fig. 20 -Saturated power output, saturation gain and overall efficiency as a function of frequency for the sixth experimental 100 watt traveling-wave tube.

17373

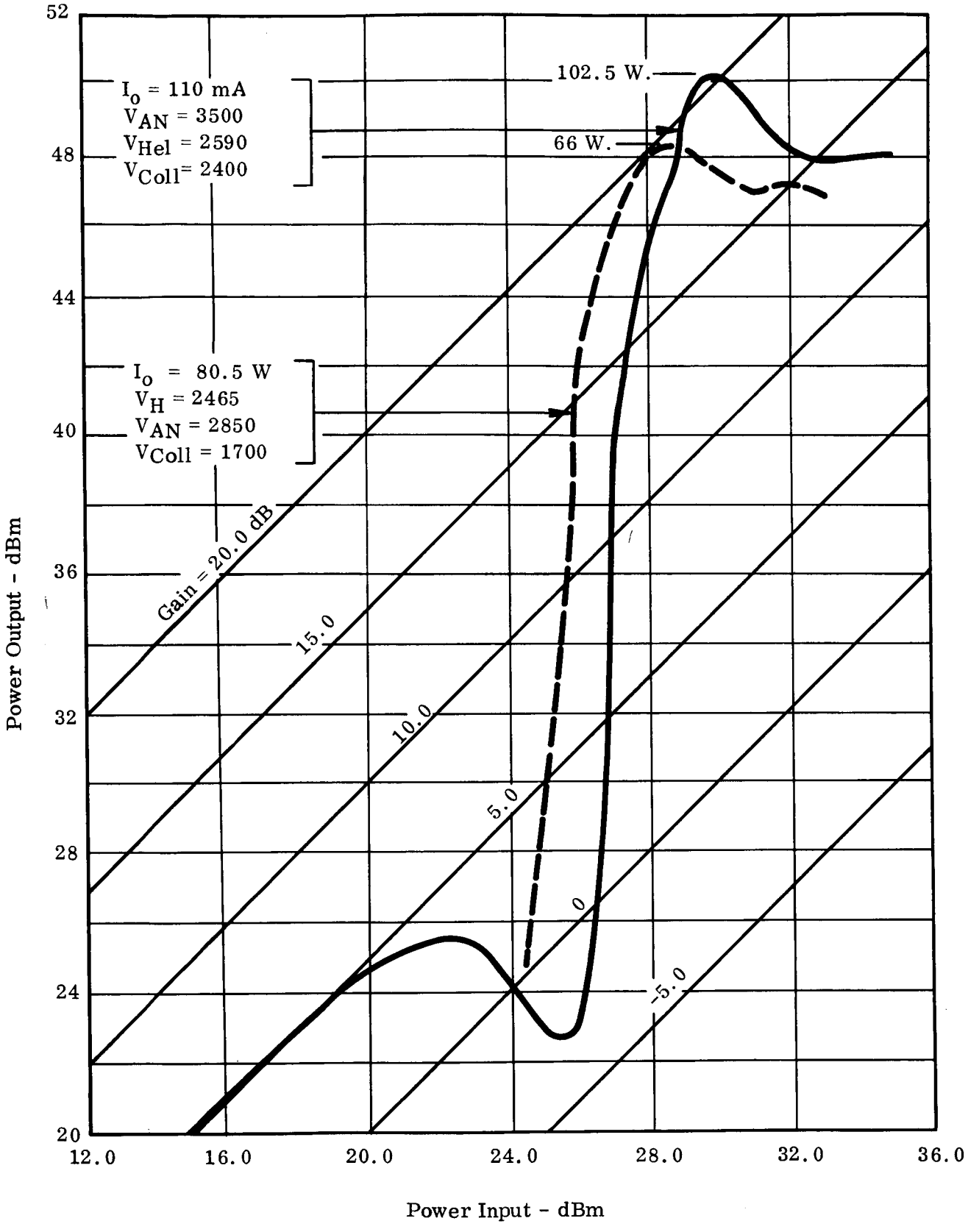

Fig. 21 - Power output vs. power input for the conditions of 66 and 102 watts for WJ-395 S/N 6. Frequency = 2.3 GHz.

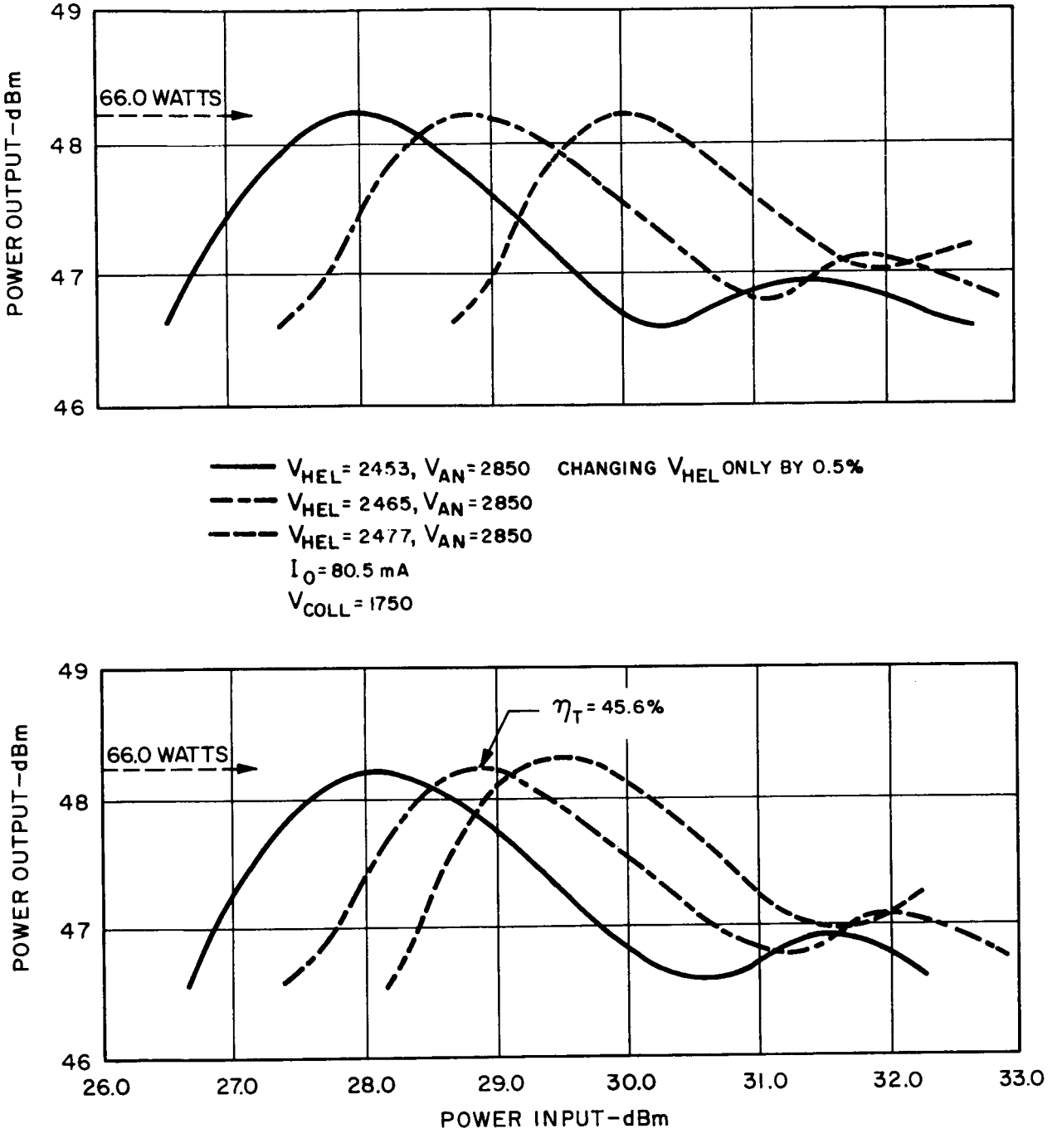

Fig. 22 - Detailed plot of the saturation region of the transfer curve showing effect of changing drive power and voltages on WJ-395 S/N 6 at 2.3 GHz.

17420

Conclusions on Tube S/N 6

Tube S/N 6 demonstrated the best beam efficiency of 36 percent at 100 watts that has been observed on the program to date. The depressed efficiency at 100 watts of 44.8 percent was demonstrated. The overall efficiency at 100 watts was 44.1 percent. Slightly better overall performance was obtained at 66 watts even though the beam efficiency was slightly lower.

The new collector design was also incorporated in this tube and performs essentially as calculated with a low temperature drop from hot spot to heat sink. It must yet be proven under environmental conditions in an encapsulated tube, but its mechanical design is felt to be good from an environmental standpoint.

III. PROGRAM FOR THE NEXT QUARTER

The following items will be included in the program of work for the next quarter:

1. Exploration of the effect on efficiency of additional gain beyond the attenuator.

2. Exploration of positive taper helix effects.

3. Further measurements on Tube S/N 6 under different magnetic field values.